

# Spin–valley phase diagram of the two-dimensional metal–insulator transition

O. GUNAWAN, T. GOKMEN, K. VAKILI, M. PADMANABHAN, E. P. DE POORTERE AND M. SHAYEGAN\*

Department of Electrical Engineering, Princeton University, Princeton, New Jersey 08544, USA

\*e-mail: shayegan@princeton.edu

Published online: 15 April 2007; doi:10.1038/nphys596

**The metallic behaviour of the resistivity observed at low temperatures in low-disorder, dilute, two-dimensional (2D) carrier systems is of considerable interest as it defies the scaling theory of localization in two dimensions<sup>1</sup>. Although the origin of the metallic behaviour remains unknown and controversial, there is widespread evidence that the spin degree of the freedom plays a crucial role. Here, we directly probe the role of another discrete electronic degree of freedom, namely the valley polarization. Using symmetry-breaking strain together with an in-plane magnetic field to tune the valley and spin polarizations of an AlAs 2D electron system at fixed density, we map out a spin–valley phase diagram for its metal–insulator transition. The insulating phase occurs in the quadrant where the system is sufficiently spin and valley polarized. This observation establishes the equivalent roles of spin and valley degrees of freedom in the 2D metal–insulator transition.**

The scaling theory of localization in two dimensions<sup>1</sup>, which predicts an insulating phase for two-dimensional electron systems (2DESs) with arbitrarily weak disorder, was challenged by the observation of a metallic temperature dependence ( $d\rho/dT > 0$ ) of the resistivity,  $\rho$ , in low-disorder, dilute 2DESs in Si metal–oxide–semiconductor field-effect transistors<sup>2</sup>. The metallic phase and its transition to an insulating phase as the density is lowered or the disorder is increased have subsequently become the subject of intense attention and controversy<sup>3–5</sup>. Although behaviour similar to that of ref. 2 has been reported for a wide variety of 2D carrier systems such as n-AlAs (ref. 6), n-GaAs (ref. 7), n-Si/SiGe (refs 8–10), p-GaAs (refs 11–13) and p-Si/SiGe (refs 14,15), the origin of the metallic state and its transition into the insulating phase remain major puzzles in solid-state physics.

Several experiments have demonstrated the important role of the spin degree of freedom in the 2D metal–insulator transition (MIT) problem, either in systems with a strong spin–orbit interaction<sup>13,16,17</sup>, or through the application of an external magnetic field to spin polarize the carriers<sup>9,10,18–22</sup>. The latter experiments have shown that a magnetic field applied parallel to the 2DES plane typically suppresses the metallic temperature dependence, ultimately driving the 2DES into the insulating phase as the 2DES is spin polarized. The relevance of multiple conduction-band valleys, on the other hand, is less well known. Although there have been indications that the occupation of multiple valleys may also be important<sup>9,10,23,24</sup>, there has been no direct experimental demonstration. Here, we show that the electrons' valley degree of freedom indeed plays a crucial role, analogous to that of spin. We study a metallic 2DES, confined to an AlAs quantum well, in which we can independently tune both

the spin and valley degrees of freedom while keeping the density fixed. By studying the temperature dependence of  $\rho$  at various degrees of spin and valley polarization, we map out the metal–insulator phase diagram in this system at constant density. The 2DES exhibits metallic behaviour when either the valley or spin is left fully unpolarized, and a minimum amount of both spin and valley polarization is required to enter the insulating phase.

We carried out experiments on 2DESs confined to modulation-doped, AlAs quantum wells of widths 11 and 15 nm. In these systems, the electrons occupy two conduction-band valleys of AlAs centred at the edges of the Brillouin zone along the [100] and [010] directions<sup>25,26</sup>. We denote these valleys as X and Y (Fig. 1b), according to the direction of their major axes. Each valley is characterized by a longitudinal  $m_l = 1.1m_0$  and a transverse  $m_t = 0.2m_0$  electron effective mass ( $m_0$  is the electron mass in vacuum). In our experiments, we apply external strain in the plane of the sample to tune the populations of the X and Y valleys<sup>26,27</sup>, and study the evolution of the 2DES as it becomes valley polarized. This is done by gluing the sample to one side of a stacked piezoelectric actuator with the sample's [100] crystal orientation aligned with the piezo's poling direction (Fig. 1a). When a voltage bias,  $V_{PZ}$ , is applied to the piezo stack, it expands (shrinks) along the [100] direction for  $V_{PZ} > 0$  ( $V_{PZ} < 0$ ) and shrinks (expands) in the [010] direction, thus inducing a symmetry-breaking strain,  $\epsilon$ , in the sample plane. Here, we define strain as  $\epsilon = \epsilon_{[100]} - \epsilon_{[010]}$ , where  $\epsilon_{[100]}$  and  $\epsilon_{[010]}$  are the fractional changes in the sample's size along the [100] and [010] directions. Such strain lifts the energy degeneracy between the X and Y valleys and electrons are transferred from one valley to another (Fig. 1b) while the total density stays constant. Owing to finite residual stress during the cooling of the sample and the piezo, we need a finite, cooldown-dependent  $V_{PZ}$  to attain the zero-strain condition in our experiments. We determine this  $V_{PZ}$  from our detailed Shubnikov–de Haas and coincidence measurements as detailed in ref. 27. For the data in Fig. 1, we determined the zero-strain condition to be at  $V_{PZ} = -285$  V, and have marked it in Fig. 1g by a dotted arrow. We then measured the strain, relative to the zero-strain condition, using a metal-foil strain gauge glued to the piezo's back.

Our measurements were carried out in a <sup>3</sup>He cryostat with a base temperature of 0.3 K. The piezo, with the glued sample, was mounted in this cryostat on a stage that could be tilted *in situ* to control the direction of the magnetic field with respect to the sample plane. The stage enables us to apply a perpendicular magnetic field to characterize the sample by measuring its electron density and the population of the valleys, and then rotate the sample and apply an in-plane magnetic field ( $B_{\parallel}$ ) to induce

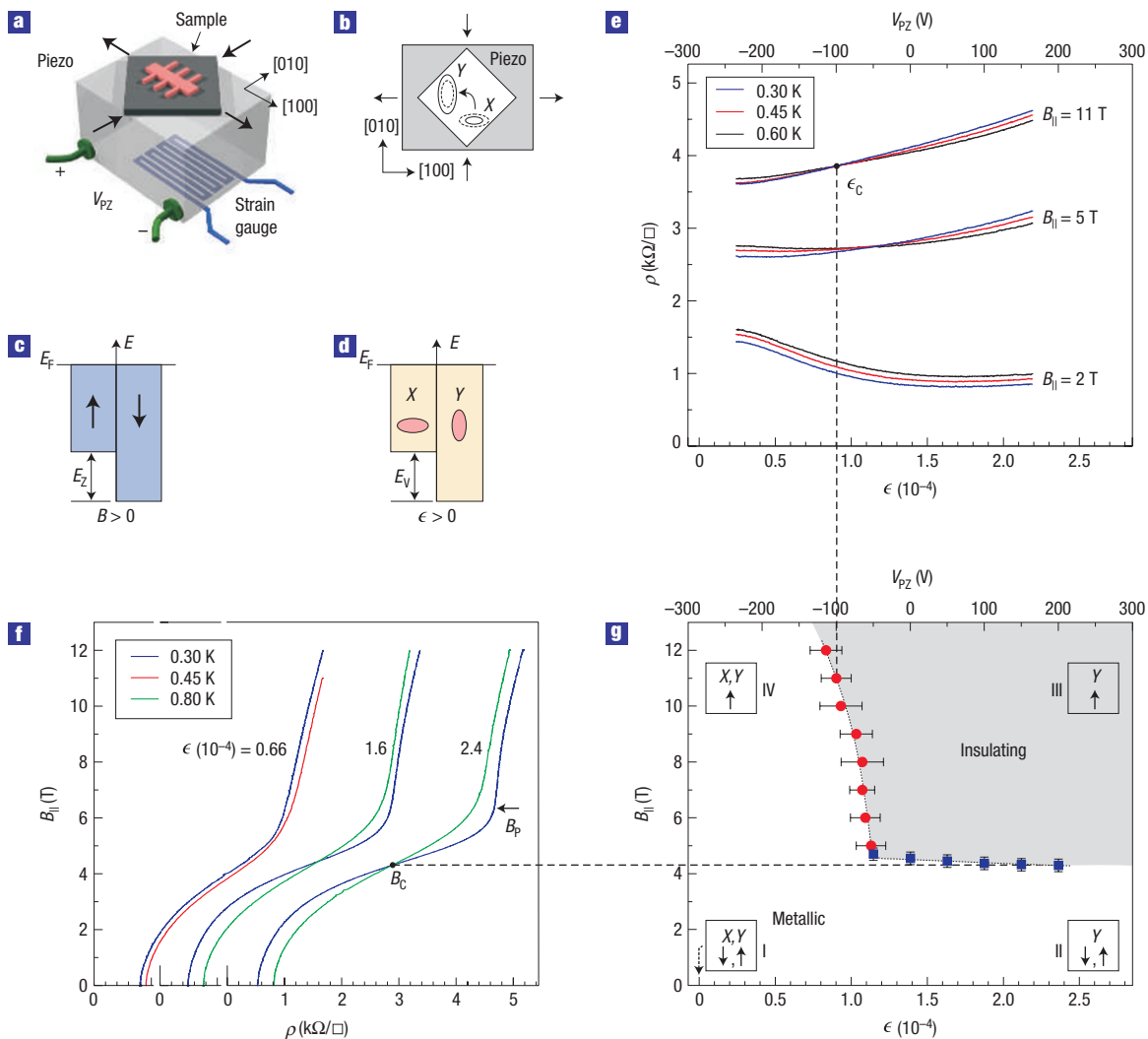


**Figure 1** Experimental set-up and the spin-valley metal-insulator phase diagram. **a**, Schematic diagram of the experimental set-up. The thick arrows indicate the situation where the sample is under tensile strain along the [100] direction and compressive strain along the [010] direction. **b**, The corresponding electron transfer from the *X* to the *Y* valley. **c,d**, Schematic diagrams showing the (Zeeman) spin and valley splittings ( $E_z$  and  $E_v$ ) with applied magnetic field or symmetry-breaking strain, respectively. **e**, Piezoresistance traces at different  $B_{||}$ . **f**, Magnetoresistance traces at various values of strain;  $B_{||}$  is applied along the [100] direction. **g**, The metal-insulator phase diagram spanning the four possible combinations of spin and valley occupation, indicated as insets at the four corners. The dotted arrow at  $\epsilon = 0$  ( $V_{pz} = -285$  V) marks the piezo bias at which the valleys are equally occupied at  $B_{||} = 0$ . The circles and squares represent the critical points  $\epsilon_c$  and  $B_c$ , deduced from temperature-dependent traces of **e** and **f**, respectively; the error bars reflect the uncertainties in determining  $\epsilon_c$  and  $B_c$ . The dotted line, delineating the phase boundary, is a guide to the eye. The sample is an 11-nm-wide AlAs quantum well with a density of  $2.5 \times 10^{11} \text{ cm}^{-2}$  and mobility (at  $\epsilon = 0$ ,  $B_{||} = 0$ , and  $T = 0.3$  K) of  $3.6 \text{ m}^2 \text{ V}^{-1} \text{ s}^{-1}$ .

Zeeman spin splitting and eventually spin-polarize the system. As schematically illustrated in Fig. 1c,d, in our experiments  $B_{||}$  and strain play analogous roles as they enable us to tune the spin and valley polarization of the 2DES, respectively.

The strain versus  $B_{||}$  phase diagram of Fig. 1g captures our main observation. The origin in this figure, where  $\epsilon$  and  $B_{||}$  are both equal to zero, represents the condition where the electrons are distributed equally between the *X* and *Y* valleys and have zero spin polarization. The opposite limit, where the 2DES is fully valley and spin polarized, is reached in the upper right corner of this diagram (quadrant III) for sufficiently large values of strain and  $B_{||}$ . In our experiments, we measure the temperature dependence of  $\rho$  as either of the two parameters  $\epsilon$  or  $B_{||}$  is kept constant and the other is swept to either spin or valley polarize the 2DES. Examples are shown in Fig. 1f, where  $\rho$  versus  $B_{||}$  traces are shown for two temperatures at

three values of strain. For  $\epsilon$  equal to  $1.6 \times 10^{-4}$  and  $2.4 \times 10^{-4}$ , the traces show that at low  $B_{||}$  the 2DES exhibits metallic behaviour ( $d\rho/dT > 0$ ), whereas above a critical field ( $B_c$ ) the behaviour turns insulating ( $d\rho/dT < 0$ ). These critical fields are marked by blue squares in Fig. 1g. The traces at  $\epsilon = 0.66 \times 10^{-4}$ , on the other hand, show that the 2DES remains metallic in the entire range of applied  $B_{||}$ . In Fig. 1e, we show traces where  $B_{||}$  is kept fixed while strain is swept continuously. Here, we see that at small values of  $B_{||}$  (for example, 2 T), the sample exhibits metallic behaviour in the entire range of  $\epsilon$ , whereas at larger  $B_{||}$ , the metallic behaviour at low  $\epsilon$  changes to insulating above a  $B_{||}$ -dependent critical  $\epsilon_c$ . These  $\epsilon_c$  are represented by red circles in Fig. 1g. The blue squares and red circles in Fig. 1g therefore define the boundary between the metallic and insulating phases of this 2DES. Figure 1g qualitatively establishes that, at a density  $n = 2.5 \times 10^{11} \text{ cm}^{-2}$ , this 2DES exhibits

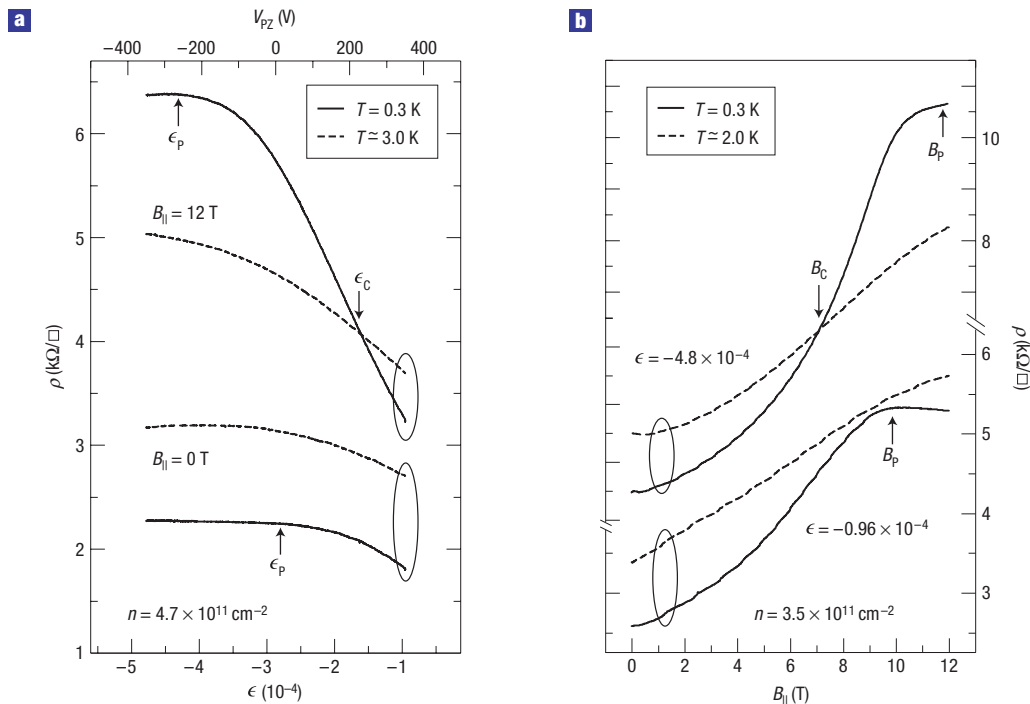


**Figure 2** Data for a 15-nm-wide AlAs quantum well sample. **a**, Piezoresistance traces at  $B_{\parallel} = 0$  T, where the 2DES is spin unpolarized, and  $B_{\parallel} = 12$  T, where it is (almost) fully spin polarized. **b**, Magnetoresistance traces at  $\epsilon = -0.96 \times 10^{-4}$ , where the 2DES is only slightly valley polarized, and  $\epsilon = -4.8 \times 10^{-4}$ , where it is fully valley polarized.

a metallic behaviour unless there is a significant amount of spin and valley polarization (quadrant III).

Several features of the data in Fig. 1e–g are noteworthy. The traces in Fig. 1f, for example, exhibit a large positive magnetoresistance, implying that, as the 2DES is made more spin polarized, its resistivity increases. This increase in  $\rho$  has been largely attributed to the loss of screening of the ionized impurities<sup>23,28</sup> and/or modification of the spin exchange interaction<sup>5</sup> on spin polarization of the 2DES. We see a more subtle dependence of  $\rho$  on valley polarization (Fig. 1e). At small  $B_{\parallel}$ , when the spins are not polarized,  $\rho$  decreases with increasing valley polarization. This is because we are measuring  $\rho$  along the [100] direction (Fig. 1a) and transferring electrons into the Y valley, which has a smaller effective mass and therefore larger mobility along the [100] direction. However, at sufficiently high  $B_{\parallel}$ , when the electrons are nearly or fully spin polarized, the data in Fig. 1e show that  $\rho$  increases with strain even though electrons are transferred into the higher mobility Y valley. This observation suggests that the screening of impurity potentials also becomes weaker with valley polarization, consistent with the theoretical calculations<sup>23</sup>, but we cannot rule out that changes in interaction, similar to the spin case<sup>5</sup>, can also play a role. No matter what the cause of increasing  $\rho$ , experimentally it is clear from Fig. 1e,f that, at a fixed low temperature,  $\rho$  is largest in the insulating (III-rd) quadrant of Fig. 1g where the 2DES is most spin and valley polarized. We emphasize that the 2DES density remains constant for all of the data shown in Fig. 1.

The above observations are further amplified by our measurements, carried out in a separate cooldown, on another AlAs sample (15 nm well width). The data are shown in Fig. 2. In this cooldown, the zero-strain condition was at a large positive  $V_{PZ} = 525$  V, so we were able to reach large compressive strain values ( $\epsilon < 0$ ) along the [100] direction and study the transport

properties as the electrons are transferred into the X valley. Overall, the data are similar to those shown in Fig. 1e,f: when the 2DES is spin or valley degenerate, its metallic behaviour survives as it is made fully valley or spin polarized (bottom sets of traces in Fig. 2). On the other hand, when the 2DES is already significantly spin (or valley) polarized, its metallic behaviour turns insulating as we valley (or spin) polarize it (top sets of traces in Fig. 2). Moreover, the piezoresistance data, shown in Fig. 2a, show that  $\rho$  increases as this charge transfer occurs even at  $B_{\parallel} = 0$ . This is because both the valley polarization and the smaller mobility (along the current direction, that is, [100]) of the X valley to which the electrons are transferred, lead to a rise in  $\rho$ . For completeness, in Fig. 2b we show the magnetoresistivity of the sample for different values of strain. The remarkable similarity of the data in Fig. 2a,b attests to the equivalent roles that the spin and valley degrees of freedom play in the MIT problem. Finally, from our measurements in the low-temperature regime ( $0.3 < T < 0.8$  K), we determined the boundaries between the metallic and insulating phases for the 15 nm quantum well sample of Fig. 2 at a density of  $4.7 \times 10^{11} \text{ cm}^{-2}$ : as expected for this higher density, the boundary is pushed to larger values of  $B_{\parallel} \simeq 10$  T and  $|\epsilon| \simeq 2 \times 10^{-4}$  compared with Fig. 1g.

The data in Figs 1 and 2 reveal yet another important clue regarding the 2D MIT. In Figs 1f and 2b, we observe that the positive magnetoresistivity nearly saturates at high fields, beyond a field  $B_p$ , as marked in Figs 1f and 2b. The field  $B_p$  represents the magnetic field beyond which the 2DES is fully spin-polarized<sup>19–22,28,29</sup>. The fields  $B_C$  and  $B_p$  are close to each other but, as pointed out by Tutuc *et al.*<sup>22</sup>, the fact that  $B_C < B_p$  implies that the transition to the insulating phase occurs not at the full spin-polarization field but rather when the population of minority spin electrons drops below a threshold value. We find that the situation is also similar for the onset of insulating

behaviour with valley polarization: as seen in Fig. 2a, the 2DES turns insulating at a critical strain ( $\epsilon_c$ ) that is smaller than the strain value at which the system becomes fully valley polarized ( $\epsilon_p$ ). (We experimentally determine  $\epsilon_p$  from the saturation of the piezoresistance, as observed in Fig. 2a, as well as careful measurements of the Shubnikov–de Haas oscillations and ‘valley-coincidence’ measurements, some of which are described in ref. 27.) Evidently, the magnitude of spin and valley polarization needed to turn the 2DES insulating is system specific as it depends on the disorder: for a sufficiently disordered system at very low densities, the 2D system is insulating even in the absence of spin or valley polarization.

Next, we note that the phase boundary denoted by the red circles in Fig. 1g is not vertical but shows a dependence on  $B_{\parallel}$ . This simply reflects the fact that, owing to the finite thickness of the electron layer, the energies of the  $X$  and  $Y$  valleys slightly shift with respect to each other as  $B_{\parallel}$  increases. The shift occurs because the parallel field couples to the orbital motion of the electrons<sup>30</sup> and changes the confinement energies of the  $X$  and  $Y$  valleys. As  $X$  and  $Y$  valleys have anisotropic Fermi contours that are orthogonal to each other, the parallel field, which is applied along the major axis of one valley ( $X$ ) and perpendicular to the other ( $Y$ ), couples differently to these valleys, causing a slight shift in their relative energies. We carried out experiments in tilted magnetic fields and, by carefully monitoring the Landau levels for the  $X$  and  $Y$  valleys as a function of  $B_{\parallel}$ , measured the shift between the energies of these valleys. Correcting for this shift, the boundary between quadrants III and IV becomes nearly vertical.

Our experimental results demonstrate that an AlAs 2DES, which exhibits metallic behaviour when it is valley or spin degenerate, turns into an insulator when the valleys and spins are both sufficiently polarized. The insulating phase has the largest resistivity at a given low temperature. The data establish experimentally the equivalence of the valley and spin degrees of freedom in the 2D MIT problem. We can interpret our data in a picture where temperature-dependent screening and disorder are responsible for the metallic behaviour and the MIT transition<sup>4,23</sup>. On the basis of studies of the role of spin, it has been suggested by several groups that temperature-dependent scattering and screening are responsible for the apparent metallic behaviour observed in 2D systems at finite temperatures<sup>4,13,16,17,21–23</sup>. When a dilute 2D system is spin and/or valley unpolarized, there is a strong and effective screening of the long-range Coulomb potential of the ionized impurities. The strong dependence of this screening on temperature leads to a metallic dependence of the resistance in a finite range of temperatures. Polarizing the 2D system weakens the screening and enhances the effective disorder, leading to a rise in the resistance and a ‘weakening’ of the metallic temperature dependence. If the disorder is sufficiently increased, either by polarizing the system or by lowering the density, the screening breaks down, leading to a percolation MIT<sup>4</sup>. Our data presented here are consistent with such an explanation. However, we cannot rule out that other mechanisms, for example, electron–electron interaction as described in ref. 5, might also be playing an important role.

Received 31 October 2006; accepted 19 March 2007; published 15 April 2007.

## References

- Abrahams, E., Anderson, P. W., Licciardello, D. C. & Ramakrishnan, T. V. Scaling theory of localization: Absence of quantum diffusion in two dimensions. *Phys. Rev. Lett.* **42**, 673–676 (1979).
- Kravchenko, S. V., Kravchenko, G. V., Furneaux, J. E., Pudalov, V. M. & D’Iorio, M. Possible metal-insulator transition at  $B = 0$  in two dimensions. *Phys. Rev. B* **50**, 8039–8042 (1994).
- Kravchenko, S. V. & Sarachik, M. P. Metal-insulator transition in two-dimensional electron systems. *Rep. Prog. Phys.* **67**, 1–44 (2004).
- Das Sarma, S. & Hwang, E. H. The so-called two dimensional metal-insulator transition. *Solid State Commun.* **135**, 579–590 (2005).
- Zala, G., Narozhny, B. N. & Aleiner, I. L. Interaction corrections at intermediate temperatures: Magnetoresistance in a parallel field. *Phys. Rev. B* **65**, R20201 (2001).
- Papadakis, S. J. & Shayegan, M. Apparent metallic behavior at  $B = 0$  of a two-dimensional electron system in AlAs. *Phys. Rev. B* **57**, R15068–R15071 (1998).
- Hanein, Y. *et al.* Observation of the metal-insulator transition in two-dimensional n-type GaAs. *Phys. Rev. B* **58**, R13338–R13340 (1998).
- Lai, K., Pan, W., Tsui, D. C. & Xie, Y.-H. Observation of the apparent metal-insulator transition of high mobility two-dimensional electron system in SiGe heterostructure. *Appl. Phys. Lett.* **84**, 302–304 (2004).
- Lai, K. *et al.* Two-dimensional metal insulator transition and in-plane magnetoresistance in a high-mobility strained Si quantum well. *Phys. Rev. B* **72**, R81313 (2005).
- Okamoto, T., Ooya, M., Hosoya, K. & Kawaji, S. Spin polarization and metallic behavior in a silicon two-dimensional electron system. *Phys. Rev. B* **69**, R41202 (2004).
- Hanein, Y. *et al.* The metallic-like conductivity of a two-dimensional hole system. *Phys. Rev. Lett.* **80**, 1288–1291 (1998).
- Simmons, M. Y. *et al.* Metal-insulator transition at  $B = 0$  in a dilute two dimensional GaAs–AlGaAs hole gas. *Phys. Rev. Lett.* **80**, 1292–1295 (1998).
- Murzin, S. S., Dorozhkin, S. I., Landwehr, G. & Gossard, A. C. Effect of hole-hole scattering on the conductivity of the two-component 2D hole gas in GaAs/AlGaAs heterostructures. *JETP Lett.* **67**, 113–119 (1998).
- Lam, J., D’Iorio, M., Brown, D. & Lafontaine, H. Scaling and the metal-insulator transition in Si/SiGe quantum wells. *Phys. Rev. B* **56**, R12741–R12743 (1997).
- Coleridge, P. T., Williams, R. L., Feng, Y. & Zawadzki, P. Metal-insulator transition at  $B = 0$  in p-type SiGe. *Phys. Rev. B* **56**, R12764–R12767 (1997).
- Papadakis, S. J., De Poortere, E. P., Manoharan, H. C., Shayegan, M. & Winkler, R. The effect of spin splitting on the metallic behavior of a two-dimensional system. *Science* **283**, 2056–2058 (1999).
- Yaish, Y. *et al.* Effect of hole-hole scattering on the conductivity of the two-component 2D hole gas in GaAs/AlGaAs heterostructures. *Phys. Rev. Lett.* **84**, 4954–4957 (2000).
- Simonian, D., Kravchenko, S. V., Sarachik, M. P. & Pudalov, V. M. Magnetic field suppression of the conducting phase in two dimensions. *Phys. Rev. Lett.* **79**, 2304–2307 (1997).
- Okamoto, T., Hosoya, K., Kawaji, S. & Yagi, A. Spin degree of freedom in a two-dimensional electron liquid. *Phys. Rev. Lett.* **82**, 3875–3878 (1999).
- Yoon, J., Li, C. C., Shahar, D., Tsui, D. C. & Shayegan, M. Parallel magnetic field induced transition in transport in the dilute two-dimensional hole system in GaAs. *Phys. Rev. Lett.* **84**, 4421–4424 (2000).
- Papadakis, S. J., De Poortere, E. P., Shayegan, M. & Winkler, R. Anisotropic magnetoresistance of two-dimensional holes in GaAs. *Phys. Rev. Lett.* **84**, 5592–5595 (2000).
- Tutuc, E., De Poortere, E. P., Papadakis, S. J. & Shayegan, M. In-plane magnetic field-induced spin polarization and transition to insulating behavior in two-dimensional hole systems. *Phys. Rev. Lett.* **86**, 2858–2861 (2001).
- Das Sarma, S. & Hwang, E. H. Low-density finite-temperature apparent insulating phase in two-dimensional semiconductor systems. *Phys. Rev. B* **72**, 205303 (2005).
- Punnoose, A. & Finkelstein, A. M. Metal-insulator transition in disordered two-dimensional electron system. *Science* **310**, 289–291 (2005).
- De Poortere, E. P. *et al.* Enhanced electron mobility and high order fractional quantum Hall states in AlAs quantum wells. *Appl. Phys. Lett.* **80**, 1583–1585 (2002).
- Shayegan, M. *et al.* Low-temperature, in situ tunable, uniaxial stress measurements in semiconductors using a piezoelectric actuator. *Appl. Phys. Lett.* **83**, 5235–5237 (2003).
- Gunawan, O. *et al.* Valley susceptibility of an interacting two-dimensional electron system. *Phys. Rev. Lett.* **97**, 186404 (2006).
- Dolgoplov, V. T. & Gold, A. Magnetoresistance of a two-dimensional electron gas in a parallel magnetic field. *JETP Lett.* **71**, 27–30 (2000).
- Shkolnikov, Y. P., Vakili, K., De Poortere, E. P. & Shayegan, M. Dependence of spin susceptibility of a two-dimensional electron system on the valley degree of freedom. *Phys. Rev. Lett.* **92**, 246804 (2004).
- Tutuc, E., Melinte, S., De Poortere, E. P., Shayegan, M. & Winkler, R. Role of finite layer thickness in spin polarization of GaAs two-dimensional electrons in strong parallel magnetic fields. *Phys. Rev. B* **67**, R241309 (2003).

## Acknowledgements

We thank the NSF and ARO for support and Y. P. Shkolnikov, E. Tutuc and K. Lai for illuminating discussions.

Correspondence and requests for materials should be addressed to M.S.

## Competing financial interests

The authors declare no competing financial interests.

Reprints and permission information is available online at <http://npg.nature.com/reprintsandpermissions/>